2001

Measurement of the hyperfine structure of the 4d2D 3/2,5/2 levels and isotope shifts of the 4p2p 3/2 ? 4d2D3/2 and 4p2p 3/2 ? 4d2D5/2 transitions in gallium 69 and 71

Steven J. Rehse
University of Windsor

W.M. Fairbank Jr.

S.A. Lee

Measurement of the hyperfine structure of the $4d^2D_{3/2,5/2}$ levels and isotope shifts of the $4p^2P_{3/2} \rightarrow 4d^2D_{3/2}$ and $4p^2P_{3/2} \rightarrow 4d^2D_{5/2}$ transitions in gallium 69 and 71

Steven J. Rehse, William M. Fairbank, Jr., and Siu Au Lee

Department of Physics, Colorado State University, Ft. Collins, Colorado 80523

(Received June 19, 2000; revised manuscript received January 2, 2001

The hyperfine structure of the $4d^2D_{3/2,5/2}$ levels of ^{69,71}Ga is determined. The $4p^2P_{3/2} \rightarrow 4d^2D_{3/2}$ (294.50-nm) and $4p^2P_{3/2} \rightarrow 4d^2D_{5/2}$ (294.45-nm) transitions are studied by laser-induced fluorescence in an atomic Ga beam. The hyperfine A constant measured for the $4d^2D_{5/2}$ level is 77.3 ± 0.9 MHz for ^{69}Ga and 97.9 ± 0.7 MHz for ^{71}Ga (3σ errors). The A constant measured for the $4d^2D_{3/2}$ level is -36.3 ± 2.2 MHz for ^{69}Ga and -46.2 ± 3.8 MHz for ^{71}Ga. These measurements correct sign errors in the previous determination of these constants. For ^{69}Ga the hyperfine B constants measured for the $4d^2D_{5/2}$ and the $4d^2D_{3/2}$ levels are 5.3 ± 4.1 MHz and 4.6 ± 4.2 MHz, respectively. The isotope shift is determined to be 114 ± 8 MHz for the $4p^2P_{3/2} \rightarrow 4d^2D_{3/2}$ transition and 115 ± 7 MHz for the $4p^2P_{3/2} \rightarrow 4d^2D_{5/2}$ transition. The lines of ^{71}Ga are shifted to the blue. This is in agreement with previous measurement.

OCIS codes: 020.2930, 020.3260, 300.2530, 300.6210.

1. INTRODUCTION

In the past several years, the use of neutral atomic beams to fabricate nanoscale features has become an active area of research.[1] Neutral atoms are attractive because of their small de Broglie wavelengths (<1 nm) and because the atoms have internal energy levels that can be accessed with lasers. It is possible to optically manipulate the atoms with laser light that is tuned close to an atomic-transition frequency.[2] If a standing-wave laser beam is positioned directly over a substrate, the atoms traveling through the laser beam experience a periodic light force and are focused into narrow lines during deposition onto the substrate.[3] Several atomic species have been optically focused, including sodium,[3,4] chromium,[5–7] cesium,[8] and aluminum.[9]

It is well known that quantum effects can be used to tailor the optical and the electronic properties of semiconductor heterostructures with nanometer-scale features. In semiconductor lasers the use of multiple quantum wells has led to improved laser performance. The ability to manipulate the lateral density of the Group III atoms during molecular-beam-epitaxy growth of a III–V semiconductor heterostructure offers an exciting possibility for fabricating such nanometer-scale features. The optical focusing of gallium (Ga) could be one method for achieving such a molecular-beam-epitaxy growth scheme.[10]

A transition between specific hyperfine levels of a ground state and an excited state is used in this optical focusing. Therefore an accurate knowledge of the hyperfine structure of both energy levels is necessary. Of interest to us is the Ga $4p^2P_{3/2} \rightarrow 4d^2D_{5/2}$ transition at 294.45 nm (for optical cooling and focusing) and the nearby $4p^2P_{3/2} \rightarrow 4d^2D_{3/2}$ transition at 294.50 nm. The $4p^2P_{3/2}$ level has been studied extensively, and the hyperfine constants are well known.[11] There has been one previous measurement of the structure of the 4^2D levels by Weber *et al.*, who used resonant Doppler-free two-photon laser spectroscopy.[12] However, the reported 4^2D hyperfine constants did not provide qualitative agreement with our laser-induced fluorescence spectra. This prompted our study of the two Ga transitions.

Ga has two stable isotopes: ^{69}Ga (60.4%) and ^{71}Ga (39.6%), both with nuclear spin $I = 3/2$. The lower energy state of the transitions of interest is the metastable state $4p^2P_{3/2}$, which lies 0.103 eV above the $4p^2P_{1/2}$ ground state.[13] With an oven source operating at typical temperatures of 1200 °C, approximately 47% of the atoms in a thermal beam will be in the $^2P_{3/2}$ state.

Hyperfine energy-level splitting is a result of the interaction between valence electrons and the nucleus. The hyperfine A and B constants represent the interactions of the electromagnetic field produced at the nucleus by the electrons with the nuclear magnetic dipole moment and with the nuclear electric quadrupole moment, respectively. The shift of a state with total angular momentum F from the unperturbed energy is given by[14]

$$\Delta E = \frac{A}{2}[F(F+1) - J(J+1) - I(I+1)] + \frac{B}{4}\frac{[\frac{3}{2}K(K+1) - 2J(J+1)I(I+1)]}{J(2J-1)I(2I-1)}, \quad (1)$$

where J is the total electronic angular momentum, I is the nuclear spin, and $K = F(F+1) - J(J+1) - I(I$

0740-3224/2001/060855-06$15.00

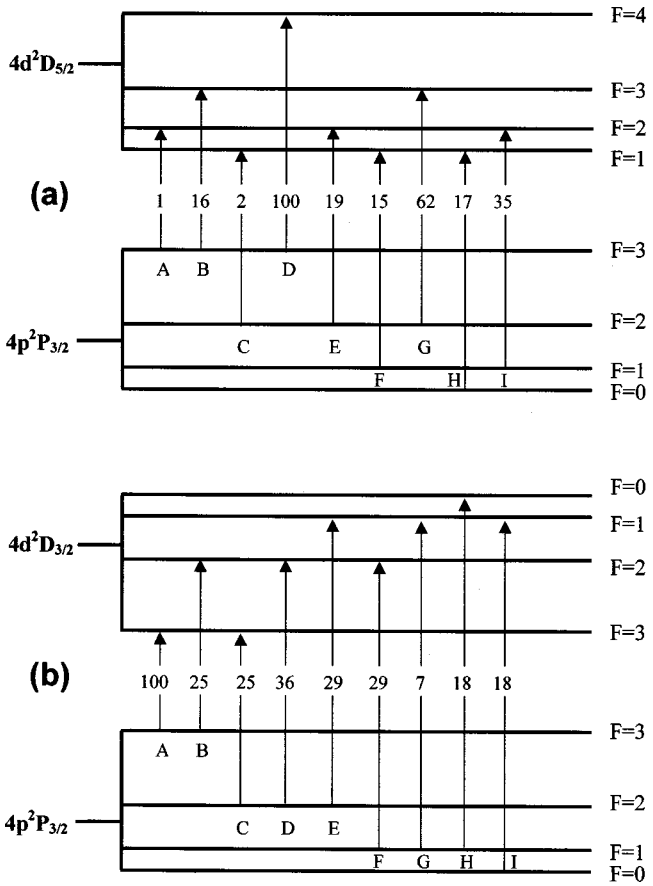

Fig. 1. Diagrams of the upper and the lower levels of the two Ga transitions studied in this paper: (a) the $4p^2P_{3/2} \rightarrow 4d^2D_{5/2}$ transition and (b) the $4p^2P_{3/2} \rightarrow 4d^2D_{3/2}$ transition. The letters (A, B, C, ...) identify particular transitions allowed by use of linearly polarized laser excitation. The numbers indicate the relative theoretical intensities of the transitions.

+ 1). The hyperfine splittings of the upper and the lower states in both transitions for Ga are shown schematically in Fig. 1.

2. EXPERIMENTAL METHODS

Spectroscopy of the two transitions required a tunable UV laser source near 294.5 nm. A 5-W laser at 532 nm was used to pump a cw single-frequency tunable dye laser producing a 500-kHz-linewidth beam at 589 nm.[15] The UV laser light was generated by frequency doubling the dye laser in an external ring cavity. The resonant cavity consisted of an asymmetric bow-tie configuration with a nonlinear crystal at one of the waists. The doubling crystal was a 1 mm × 1 mm × 20 mm Brewster-cut ammonium dihydrogen arsenate crystal heated to approximately 34 °C for 90° phase matching.[16] The temperature of the crystal was stabilized to better than ±0.01 °C. A dichroic beam splitter inserted in the cavity was used to reflect the frequency-doubled UV laser light out of the cavity. The dye-laser power into the cavity was between 300 and 400 mW, and typical UV laser powers generated were 1–3 mW. The relatively high loss in the ammonium dihydrogen arsenate crystal (~2%/cm) and cavity parameters not configured for optimal performance limited power buildup in this cavity to somewhere in the range of 6–10.

The wavelength of the fundamental laser was determined by the lambda meter: a traveling Michelson interferometer with a frequency-stabilized He–Ne reference laser.[17] As the dye laser was tuned, the frequency interval was monitored by a temperature-stabilized 1-m confocal Fabry–Perot cavity with a free spectral range of 74.227(36) MHz.[18]

A beam of Ga atoms was generated by a resistively heated effusive oven source with a 0.8-mm-diam aperture hole. The oven source and the atomic beam were housed in a diffusion-pumped vacuum system at $\sim 2 \times 10^{-6}$ Torr ($\sim 1 \times 10^{-5}$ Torr when the oven was operating). The oven was operated at approximately 1200 °C, as determined by an optical pyrometer. A 0.7 mm × 1.0 mm aperture slit was placed in the Ga beam, 15 cm from the oven, to collimate it. The UV laser was introduced into the vacuum system through quartz Brewster windows and passed perpendicular to the Ga beam at a distance of approximately 15 cm from the collimating slit. The laser beam-waist diameter was ~1 mm, giving an intensity in the laser–atom interaction region comparable with the saturation intensity for most of the m_F components of the hyperfine levels.[19] A photomultiplier tube (PMT) located above the interaction region was used to detect the fluorescence as the UV laser frequency was scanned through the transitions. A schematic of the gallium beam source and the interaction region is given in Fig. 2.

The fluorescence spectra from the PMT as well as the fringe signal from the 1-m calibration cavity were recorded and digitized. The Fabry–Perot cavity fringe scans were used to calibrate the fluorescence spectra and check for scan nonlinearities. The UV laser power was monitored during the scans, and these data were used to correct for UV laser power fluctuations in the fluorescence

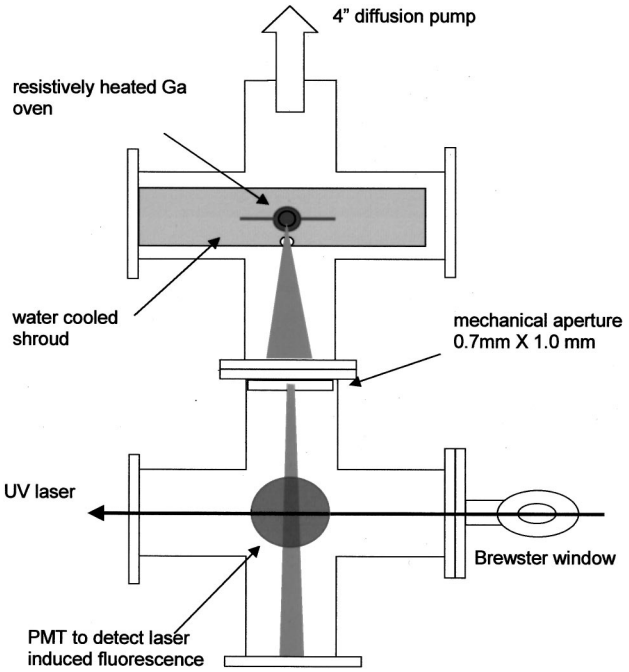

Fig. 2. Schematic of the Ga atomic-beam apparatus.

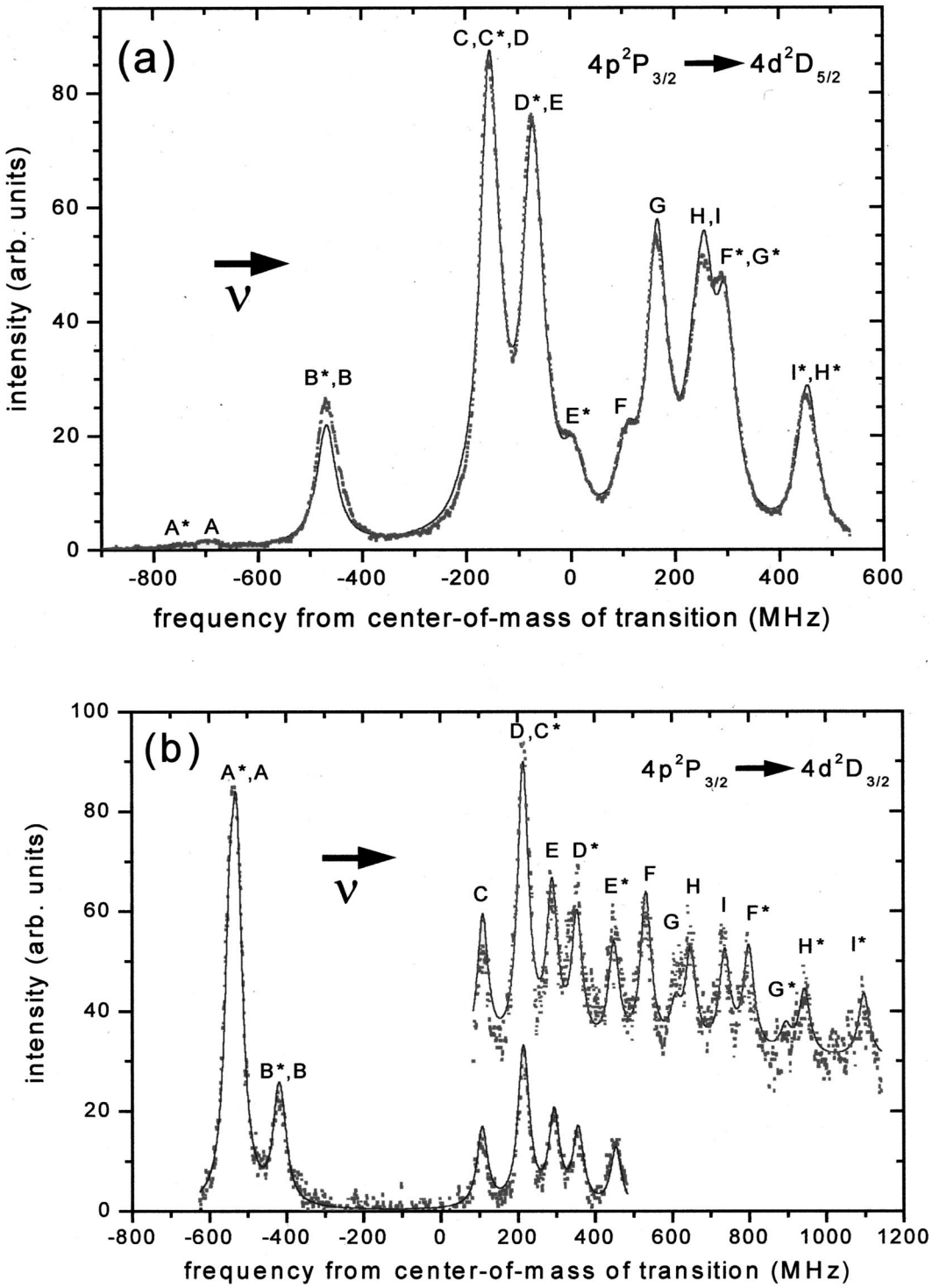

Fig. 3. Laser-induced fluorescence spectrum (dotted curve) and the fitted spectrum (solid curve) for the (a) $4p^2P_{3/2} \rightarrow 4d^2D_{5/2}$ and (b) $4p^2P_{3/2} \rightarrow 4d^2D_{3/2}$ transitions. Frequency 0 denotes the center of mass of the ^{69}Ga transition. Specific hyperfine transitions designated with a letter (A, B, C, ...) are identified in Fig. 1. Transitions designated with an asterisk (*) are from the isotope ^{71}Ga. In several instances one or more peaks overlap and are indistinguishable. In (b) the vertical scale of the blue end of the spectrum has been magnified.

spectra. Multiple spectra were taken for each transition. Typical fluorescence spectra are shown in Fig. 3. In both transitions the 18 different hyperfine components from the two Ga isotopes are not all resolved. In the case of the $4p^2P_{3/2} \rightarrow 4d^2D_{3/2}$ transition the locking range of the doubling cavity was not sufficiently broad to allow a complete fluorescence spectrum to be obtained in one continuous scan. Hence two scans were made.

3. ANALYSIS

The laser-induced fluorescence spectra were fitted with a nonlinear least-squares procedure. The hyperfine con-

stants for the $4d^2D$ states and the isotope shifts of the transitions were obtained from this analysis, whereas the constants for the $4p^2P_{3/2}$ state were obtained from Ref. (11) and were not measured. Specifically, the hyperfine A coefficients for both ^{69}Ga and ^{71}Ga, the B coefficient for ^{69}Ga, and the isotope shift were used as fitting parameters. The spectra did not have sufficient resolution to allow a separate B coefficient for ^{71}Ga to be determined independently. Therefore its value was fixed to the value for ^{69}Ga by the relation $B(^{71}\mathrm{Ga}) = 0.630 \times B(^{69}\mathrm{Ga})$, where the factor 0.630(1) is the ratio of the nuclear electric quadrupole moments determined previously.[20] The 18 hyperfine components were assumed to have Lorentzian line shapes with identical widths. Their relative intensities were fixed to the theoretical line-strength ratios (shown in Fig. 1) and the isotopic abundance ratio. Thus the line-shape width and the overall intensity were additional fitting parameters. A 42(8)-MHz linewidth was determined for the $4p^2P_{3/2} \rightarrow 4d^2D_{5/2}$ transition, and a 32(11)-MHz linewidth was found for the $4p^2P_{3/2} \rightarrow 4d^2D_{3/2}$ transition (3σ errors). The natural linewidth of the transition is 25 MHz. The residual Doppler width was less than 6 MHz and could be neglected. The difference between the natural and the fitted linewidths can be attributed to power broadening. The laser-saturation parameter (I/I_0) was 1.5 to 2.0 for the $4p^2P_{3/2} \rightarrow 4d^2D_{5/2}$ fluorescence spectrum and was 0.5 to 1.0 for the $4p^2P_{3/2} \rightarrow 4d^2D_{3/2}$ spectrum. Using these values of the saturation parameter, our fitted values for the linewidths agree well with the estimated power-broadened linewidths. The fitted spectra are shown in Fig. 3 as solid curves.

Other fitting procedures were also investigated. The peak intensities of some of the strongest lines were allowed to vary independently. A lower χ^2 was obtained, but the hyperfine-constant results did not change significantly with these additional parameters. Fitting was also attempted without locking the ratio of the B constants; however, no meaningful value for $B(^{71}\mathrm{Ga})$ could be determined. These other procedures were not used to determine the final results.

4. RESULTS

The three hyperfine parameters and the isotope shifts, determined by averaging over seven scans of the $4p^2P_{3/2} \rightarrow 4d^2D_{5/2}$ transition and three pairs of scans of the $4p^2P_{3/2} \rightarrow 4d^2D_{3/2}$ transition, are given in Table 1. Previously published results are given for comparison.

The agreement with the absolute value of the published A values is excellent. The difference in sign, but not in magnitude, of the A coefficients between our investigation and Ref. 12 required further investigation. The laser-scan direction was checked carefully with the lambda meter and verified against known iodine transitions. Furthermore, having an A coefficient with the opposite sign in the 4^2D state would not simply reverse the positions of the spectral lines. It would completely change the locations of the components because the hyperfine structure of the ground state remains unchanged. This effect is shown in Fig. 4 for the $4p^2P_{3/2} \rightarrow 4d^2D_{5/2}$ transition. As can be seen in Fig. 4(c), an opposite sign in A cannot fit the laser-induced-fluorescence spectrum obtained in this study.

To explain the discrepancy in sign, it became necessary to examine the previous experiment in more detail. In Ref. 12, the Ga hyperfine structure was obtained with resonant Doppler-free two-photon spectroscopy, with the 4^2D state being the intermediate state. Two lasers were used to obtain resonance, one fixed and one tunable, and both counterpropagating and copropagating spectra were taken to determine the intermediate-state structure. Thus the experiment had more variables than our simple laser-induced fluorescence technique. We have fitted the spectra in Ref. 12 using our hyperfine constants. In the $4^2P_{1/2} \rightarrow 4^2D_{3/2}$ case (Fig. 2 of Ref. 12), the agreement was excellent for both the copropagating and counterpropagating spectra. For the $4^2P_{3/2} \rightarrow 4^2D_{5/2}$ transition (Fig. 3 of Ref. 12) the agreement was also excellent if we assumed that laser two was tuned. (The isotopes were also mislabeled in that figure.) In all cases the peak locations agreed to within 10 MHz. At the same time we tried the opposite signs on the A coefficients, i.e., using the results of Ref. 12. We found that regardless of which laser was tuned, there was no agreement between the calculated and the measured peak positions in all cases. The misfit was similar to the type shown in Fig. 4. Thus the signs of the A coefficients reported in Ref. 12 are incorrect.

The present study provides a significant improvement in the accuracy of the hyperfine constants and corrects sign errors in the previous determination of the A constants. The ratios of $A(^{71}\mathrm{Ga})/A(^{69}\mathrm{Ga})$ are 1.27(2) and 1.27(13) for the $4d^2D_{5/2}$ and $4d^2D_{3/2}$ levels, respectively. These numbers agree well with the ratio of the nuclear magnetic dipole moments, 1.2700(8).[20] No other measurement of the B constants has been made before this

Table 1. Experimental Values of the Hyperfine Structure Constants and the Isotope Shifts

		^{69}Ga		^{71}Ga			
Level	Source	A (MHz)	B (MHz)	A (MHz)	B (MHz)	Transition	Isotope Shift (MHz)[b]
$4d^2D_{3/2}$	This paper	−36.3(2.2)	+4.6(4.2)	−46.2(3.8)	[a]	$4p^2P_{3/2} \rightarrow 4d^2D_{3/2}$	+114(8)
	Weber *et al.*[12]	+36(2)	–	+46(3)	–		+121(10)
$4d^2D_{5/2}$	This paper	+77.3(0.9)	+5.3(4.1)	+97.9(0.7)	[a]	$4p^2P_{3/2} \rightarrow 4d^2D_{5/2}$	+115(7)
	Weber *et al.*[12]	−78(3)	–	−98(4)	–		+117(9)

[a] $B(^{71}\mathrm{Ga}) = 0.630 \times B(^{69}\mathrm{Ga})$.

[b] The convention for the sign of the isotope shift is to report a positive shift when the lines of the heavier isotope (in this case ^{71}Ga) are shifted to the blue.

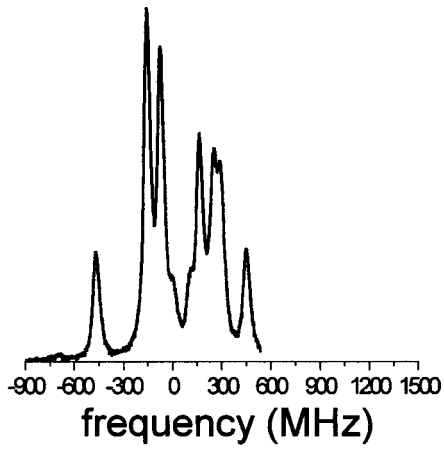

(a)

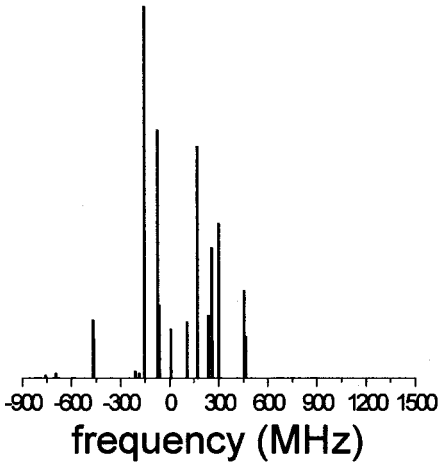

(b)

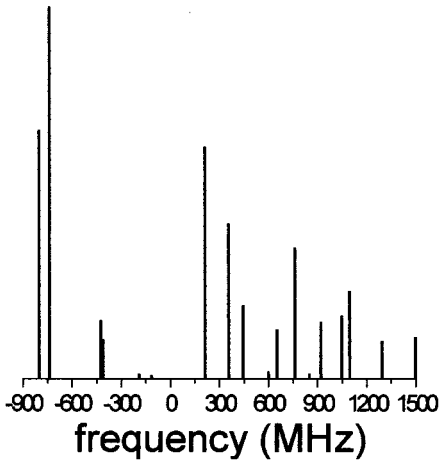

(c)

Fig. 4. (a) Laser-induced fluorescence spectrum for the $4p^2P_{3/2} \rightarrow 4d^2D_{5/2}$ transition obtained in the present study. (b) Calculated peak locations obtained with the hyperfine constants reported in this paper. (c) Calculated peak locations obtained with the hyperfine constants reported in Ref. 12.

study. The measured isotope shifts fall within the errors of the previously published values.

The uncertainties reported with our parameter values are 3σ deviations from the mean. The dominant error in the data is due to the noise of the laser-induced fluorescence signal, particularly in the $4p^2P_{3/2} \rightarrow 4d^2D_{3/2}$ transition, which had a much smaller signal. Systematic errors, e.g., frequency-scan nonlinearities, UV-laser power variations, and optical pumping effects, are small by comparison.

5. CONCLUSIONS

The hyperfine structure of the $4p^2P_{3/2} \rightarrow 4d^2D_{3/2}$ and $4p^2P_{3/2} \rightarrow 4d^2D_{5/2}$ transition in 69 and 71 Ga is investigated. The accuracy of the hyperfine A constants is significantly improved, and sign errors in the existing literature values are corrected. Values of the hyperfine B constants are also reported. The measured isotope shifts agree well with previously determined values.

ACKNOWLEDGMENT

This research was supported by the National Science Foundation under grant PHY9732498.

S. J. Rehse's e-mail address is rehse@lamar.colostate.edu.

REFERENCES AND NOTES

1. J. H. Thywissen, K. S. Johnson, R. Younkin, N. H. Dekker, K. K. Berggren, A. P. Chu, M. Prentiss, and S. A. Lee, "Nanofabrication using neutral atomic beams," J. Vac. Sci. Technol. B **15**, 2093–2100 (1997).
2. For a discussion of light forces and applications, see, for example, the following special issues: P. Meystre and S. Stenholm, eds., "The mechanical effects of light" J. Opt. Soc. Am. B **2**, 1706–1853 (1985); S. Chu and C. Wieman, eds., "Laser cooling and trapping of atoms," J. Opt. Soc. Am. B **6**, 2020–2270 (1989); J. Mlynek, V. Balykin, and P. Meystre, eds., "Optics and interferometry with atoms," Appl. Phys. B **54**, 319–485 (1992). See also *Atom Optics*, Proc. SPIE **2995**, M. G. Prentiss and W. D. Phillips eds. (SPIE, Bellingham, Washington, 1997), pp. 2–300.
3. G. Timp, R. E. Behringer, D. M. Tennant, J. E. Cunningham, M. Prentiss, and K. K. Berggren, "Using light as a lens for submicron, neutral-atom lithography," Phys. Rev. Lett. **69**, 1636–1639 (1992).
4. V. Natarajan, R. E. Behringer, and G. Timp, "High-contrast, high-resolution focusing of neutral atoms using light forces," Phys. Rev. A **53**, 4381–4385 (1996).
5. J. J. McClelland, R. E. Scholten, E. C. Palm, and R. J. Celotta, "Laser-focused atomic deposition," Science **262**, 877–880 (1993).
6. R. Gupta, J. J. McClelland, Z. J. Jabbour, and R. J. Celotta, "Nanofabrication of a two-dimensional array using laser-focused atomic deposition," Appl. Phys. Lett. **67**, 1378–1380 (1995).
7. U. Drodofsky, J. Stuhler, B. Brezger, T. Schulze, M. Drewsen, T. Pfau, and J. Mlynek, "Nanometerscale lithography with chromium atoms using light forces," Microelectron. Eng. **35**, 285–288 (1997).
8. F. Lison, H.-J. Adams, D. Haubrich, M. Kreis, S. Nowak, and D. Meschede, "Nanoscale atomic lithography with a cesium atomic beam," Appl. Phys. B **65**, 419–421 (1997).
9. R. W. McGowan, D. M. Giltner, and S. A. Lee, "Light force cooling, focusing, and nanometer-scale deposition of aluminum atoms," Opt. Lett. **20**, 2535–2537 (1995).
10. S. J. Rehse, R. W. McGowan, and S. A. Lee, "Optical manipulation of Group III atoms," Appl. Phys. B **70**, 657–660 (2000).
11. R. T. Daly, Jr., and J. H. Holloway, "Nuclear magnetic octupole moments of the stable gallium isotopes," Phys. Rev. **96**, 539–540 (1954). Specifically, the constants for the

$4^2P_{3/2}$ level are, for ^{69}Ga, $A = 190.79428(15)$ MHz and $B = 62.52247(30)$ MHz, and for ^{71}Ga, $A = 242.43395(20)$ MHz and $B = 39.39904(40)$ MHz.
12. K. H. Weber, J. Lawrenz, A. Obrebski, and K. Niemax, "High-resolution laser spectroscopy of aluminum, gallium, and thallium," Phys. Scr. **35**, 309–312 (1987).
13. C. E. Moore, *Atomic Energy Levels* (U.S. GPO, Washington, D.C., 1971), Vol. II.
14. G. T. Emery, "Hyperfine structure," in *Atomic, Molecular, and Optical Physics Handbook*, G. W. F. Drake, ed. (American Institute of Physics, Woodbury, N.Y., 1996), pp. 198–205.
15. The pump laser was a Spectra Physics Nd:YVO_4 Millenia™ laser. The tunable dye laser was a Coherent 699-21 with Rhodamine 6G dye.
16. ADA ($NH_4H_2AsO_4$) is a hygroscopic, temperature-tunable nonlinear second-harmonic-generation crystal. Our crystal was a 45° Z-cut crystal purchased from Quantum Technology, Inc. We have measured its second-harmonic-generation efficiency to be between 6×10^{-5} W/W^2 and 2×10^{-4} W/W^2. These numbers may not represent optimum second-harmonic-generation efficiency, as the focusing of the doubling cavity's waist was not optimized for this particular crystal.
17. J. L. Hall and S. A. Lee, "Interferometric real-time display of cw dye laser wavelength with sub-Doppler accuracy," Appl. Phys. Lett. **29**, 367–369 (1976).
18. L. Hlousek, S. A. Lee, and W. M. Fairbank, Jr., "Precision wavelength measurements and new experimental Lamb shifts in helium," Phys. Rev. Lett. **50**, 328–331 (1983).
19. The tunable UV laser was linearly polarized, and the saturation intensities calculated for the transitions between m_F levels of the $F = 3 \rightarrow F' = 4$ transition are 202 mW/cm^2 for the $m_F = 0 \rightarrow m_F' = 0$ transition, 215 mW/cm^2 for the $m_F = 1 \rightarrow m_F' = 1$ transition, 269 mW/cm^2 for the $m_F = 2 \rightarrow m_F' = 2$ transition, and 464 mW/cm^2 for the $m_F = 3 \rightarrow m_F' = 3$ transition. These values are typical of the other $F \rightarrow F'$ transitions as well.
20. G. H. Fuller, "Nuclear spins and moments," J. Phys. Chem. Ref. Data **5**, 835–1016 (1976).